Polarization structures in parhelic circles and in 120° parhelia

Günther P. Können and Jaap Tinbergen

Parhelic circles due to plate-oriented crystals (hence, with main axes vertical) and 120° parhelia change in position when viewed through a rotating polarizer. The parhelic circle moves vertically; its largest shift is found at an azimuthal distance between 90° and 120° from the Sun. The 120° parhelia move both vertically and horizontally. The magnitudes of the shifts are between 0.1° and 0.3°, depending on solar elevation. The mechanism is polarization-sensitive internal reflection by prism faces of the ice crystals. We outline the theory and present three visual and one instrumental observation of the displacements of these halos in polarized light. © 1998 Optical Society of America

OCIS codes: 010.1290, 010.2940, 260.5430.

1. Introduction

The polarization dependence of the refractive index of ice causes inner limbs of refraction halos to be strongly polarized.[1–4] On closer inspection, this (linear) birefringence appears to result in polarized limbs of reflection halos also. This curiosity of nature, visible as shifting positions of the parhelic circle and the 120° parhelia when viewed through a rotating polarizer, arises when the halo-generating light path includes internal reflection at a prism face.

The mechanism is as follows. Light travels through an ice crystal in one of the polarized normal crystal modes (called ordinary and extraordinary) for that direction of propagation. When light of such a normal mode is reflected at a prism face, the polarization after reflection will, in general, not correspond to one of the two normal modes for the new direction of propagation. Consequently, the intensity of the incident ray is redistributed over the two new normal modes, which results in two reflected rays following slightly different paths through the crystal. Because the two reflected rays are orthogonally polarized, this leads to a polarization dependence of the position in the sky of the resulting reflection halo.

The above splitting into two polarized components applies to both partial internal reflection and to total reflection. This means that the shift of reflection halos in polarized light is not limited to the low-intensity ray paths of partial reflection, but also occurs in the high-intensity ray paths of total reflection. This is why the shift can actually be observed in nature.

In this paper, theory and observations of the displacements in polarized light of the parhelic circle and the 120° parhelia are described. The calculations outlined in the theoretical section apply specifically to ray paths consisting of two refractions and one or two internal reflections. These ray paths provide by far the dominating contribution to the parhelic circle radiance at the azimuth of maximum shift and to that of the 120° parhelion, respectively.[5] Therefore the results of the theoretical section apply to parhelic circles and 120° parhelia as they actually appear in nature.

2. Theory

A. Polarized Components

The theory of refraction and reflection of light in birefringent crystals is described by Szivessy.[6] In this section we summarize his results to the extent that they apply to halo polarization.

Ice belongs to the hexagonal crystal class $6mm$, so an ice crystal is linearly birefringent and uniaxial. The optic axis of ice coincides with the crystallographic C axis (the crystal main axis). The ordinary index of refraction n_o ($\cong 1.31$) is 0.0014 smaller[7] than

G. P. Können is with the Royal Netherlands Meteorological Institute, P.O. Box 201, 3730 AE De Bilt, The Netherlands. J. Tinbergen is with the University of Leiden and the Netherlands Foundation for Research in Astronomy, P.O. Box 2, 7990 AA Dwingeloo, The Netherlands.

Received 6 June 1997; revised manuscript received 16 September 1997.

0003-6935/98/091457-08$15.00/0

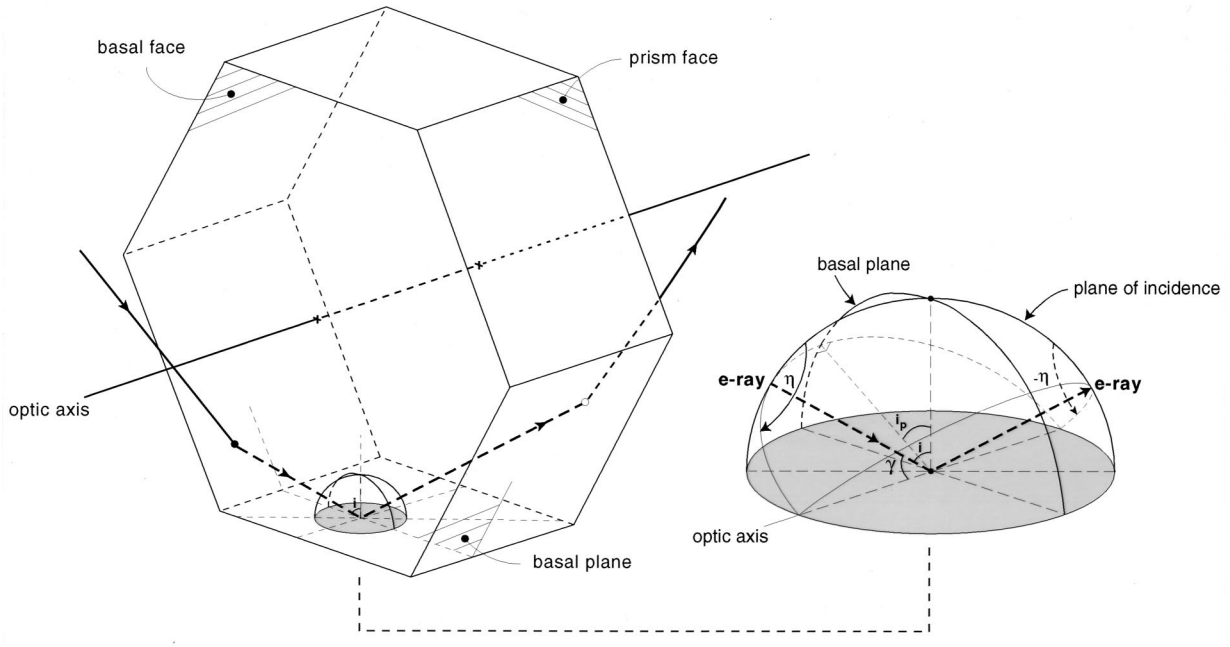

Fig. 1. Internal reflection of (the wave normal of) the *e* ray at a prism face (the ray enters and leaves the crystal through basal faces). In addition to the plane of incidence and the basal plane (the plane through the point of reflection and parallel to basal faces of the crystal), the right-hand diagram shows the planes containing the optic axis and, respectively, the incident ray and the reflected ray. The index of refraction for an *e* ray is determined by the angle γ and its polarization (electric-field vibration) is always in the plane defined by the optic axis and the ray. The angle η defines the polarization angle of the incident *e* ray with respect to the plane of incidence. The polarization angle of the reflected *e* ray is $-\eta$, which differs from that expected by the Fresnel laws of reflection. As a result, a second ray (an ordinary one, not shown) of opposite polarization is created at reflection. Its wave normal is also in the plane of incidence, but its angle of reflection differs from the angle of incidence i. Reflection of *o* rays is analogous to that of *e* rays. The angle i_p is the projection of i onto the basal plane.

the extraordinary index of refraction n_e. An unpolarized ray of light that enters an ice crystal is split into two polarized rays: an ordinary refracted ray (*o* ray) and an extraordinary ray (*e* ray). The polarization (direction of vibration of the electric field) of the *o* ray is perpendicular to the plane defined by the *o* ray and the optic axis; that of the *e* ray is parallel to the plane defined by the *e* ray and the optic axis. The wave normal of the *o* ray is subject to a refractive index of n_0; that of the *e* ray to n_{eff} is given by

$$\frac{1}{n_{\text{eff}}^2} = \frac{\sin^2\gamma}{n_o^2} + \frac{\cos^2\gamma}{n_e^2}, \tag{1}$$

where γ is the angle between the *e* ray (wave normal) and the optic axis. Note that $n_0 < n_{\text{eff}} \leq n_e$. The angle of refraction of the *e* ray is defined by Eq. (1) and Snel's[8,9] law.

The two rays follow different paths through the crystal. When the *e* ray is reflected at a crystal face and the incident polarization is inclined with respect to the plane of incidence, the polarization state of the reflected ray will generally not correspond to that of an *e* ray for that direction of propagation (Fig. 1). As a result, the intensity of the incident ray will be distributed between a reflected *e* ray that follows the usual law of reflection and a newly created *o* ray. The latter's path can be found[6] from

$$n_{\text{eff}} \sin i = n_o \sin i' \qquad (e \rightarrow o), \tag{2}$$

where i and i' are the angles of incidence and reflection, respectively, of the wave normals. For an *o* ray that is reflected, a similar argument holds, and the angle of reflection i' of the newly created *e* ray follows from

$$n_o \sin i = n_{\text{eff}} \sin i' \qquad (o \rightarrow e). \tag{3}$$

Equations (2) and (3) hold for totally reflected rays as well as for partially (internally) reflected rays.

New rays are created only during reflection at a prism face (or at a pyramidal face, which case is not considered here), but never through reflection at a basal face. The reason is that, for basal faces, the optic axis is always in the plane of incidence, and hence the polarizations of the *o* ray and the *e* ray are always at 90° and 0°, respectively, relative to the plane of incidence.

Further internal reflection at a prism face leads to additional splitting of the rays. Hence the number of *o* rays and *e* rays that travel through the crystal increases exponentially with the number of reflections. However, for a crystal that consists of basal and prism faces only, the angle γ is the same for all *e* rays and, similarly, the same for all *o* rays. As the face normal of a basal face is parallel to the optic axis, these two angles γ represent the angle of incidence at basal faces of any *e* ray and any *o* ray, respectively.

B. Parhelic Circles

We now consider plate-oriented crystals (main axes vertical) and the ray path of the parhelic circle that consists of entrance at the upper basal face, reflection at a prism face, and exit at the bottom basal face (i.e., 132 in Tape's[5] notation of the crystal faces); this path produces by far the main contribution to the circle's radiance. There are four possible sequences of polarization in this path. With the face numbers between parentheses, they are

$$(1)o(3)o(2) \equiv oo, \qquad (1)e(3)o(2) \equiv eo,$$
$$(1)o(3)e(2) \equiv oe, \qquad (1)e(3)e(2) \equiv ee. \tag{4}$$

The right-hand sides represent a shortened notation that indicates the consecutive states of the ray while traveling through the crystal. In each case, the last symbol indicates the state of the emerging ray. Because of the vertical orientation of the optic axes, *o* rays emerging from plate-oriented crystals are horizontally polarized and *e* rays are vertically polarized.

Let h_p be the elevation of the parhelic circle and h_{sun} the solar elevation. It then follows from Snel's law and from Eqs. (1)–(3) that, for any azimuth,

$$h_p = h_{\text{sun}} \qquad (oo, ee \text{ paths}),$$
$$n_o \cos h_p = n_e \cos h_{\text{sun}} \qquad (oe \text{ path}),$$
$$n_e \cos h_p = n_o \cos h_{\text{sun}} \qquad (eo \text{ path}). \tag{5}$$

Equations (5) show that idealized parhelic circles from plate-oriented crystals actually consist of three separate concentric circles: a middle circle that behaves as in isotropic crystals (weakly polarized by Fresnel losses only), a 100% horizontally polarized upper satellite circle, and a 100% vertically polarized lower satellite circle.

For parhelic ray paths involving more internal reflections, Eqs. (5) remain valid because of the constancy of the angles γ. On the other hand, a parhelic circle from column-oriented or Parry-oriented crystals (hence, with the main crystal axis horizontal) will not produce a perceptible split, as the internal reflection in the main ray path (316) takes place at a basal face.

C. Azimuthal Positions of the 120° Parhelion Components

For the 120° parhelia the most prominent ray path[5] is 1342 (Tape's notation[5]), i.e., entrance and exit at basal faces and internal reflections at two adjacent prism faces (see Fig. 2, top left). The horizontal deflection of rays during a transition from *e* rays to *o* rays or vice versa can be calculated from Eqs. (1)–(3). It can be proved that for plate-oriented crystals the projected paths of rays on the horizontal (normal) plane are subject to the following Snel-like laws:

$$n_e \sin i_p = n_o \sin i_p' \qquad (e \rightarrow o),$$
$$n_o \sin i_p = n_e \sin i_p' \qquad (o \rightarrow e), \tag{6}$$

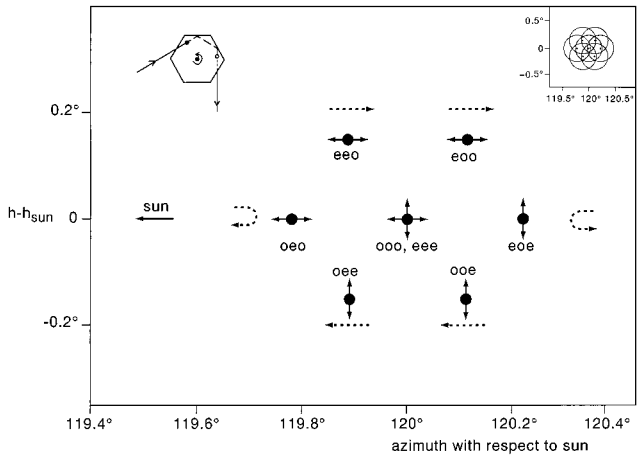

Fig. 2. Fine structure of a 120° parhelion due to birefringence. The sequences of ordinary and extraordinary rays in the light paths inside the crystal are indicated: e.g., *oeo* means ordinary–extraordinary–ordinary ray. The polarization is indicated for each spot. The virtually unpolarized central spot corresponds in position to that of the 120° parhelion in isotropic crystals. The azimuthal displacements of the six satellite spots are independent of solar elevation h_{sun}; their vertical displacement $h - h_{\text{sun}}$ in the figure corresponds to a solar elevation of 25°. The figure displays the situation in which the path of the *ooo* ray is symmetrical with respect to the crystal hexagon (projected angles of incidence of 60° for both prism faces). Rotation of the crystal about its vertical axis causes a change in azimuthal position of the six satellites; their directions are indicated (dashed arrows). The inset depicts the effect of solar-disk smearing of the spots.

where i_p is the angle of incidence projected on the horizontal plane (which is equivalent to the basal face) and i_p' is the projected angle of reflection. Equations (6) indicate that Bravais transformations of n_{eff}/n_o and n_o/n_{eff} yield Bravais refractive indices n_e/n_o and n_o/n_e, respectively, which are constants. Consequently there is no solar elevation dependency in Eqs. (6).

The combination of Eqs. (5) and (6) allows us to calculate the splitting of the idealized 120° parhelion into polarized components. Figure 2 shows the result for a fixed crystal position with a symmetrical light path of *ooo* rays ($i_p = 60°$). The 120° parhelion is split into seven components: one virtually unpolarized central spot at the normal 120° parhelion position and six polarized satellite spots around it. Rotation of the crystal about its vertical axis does not affect the position of the central spot or the elevations of the six satellites, but it does affect the azimuths of the latter. Equations (6) indicate that the azimuths of the *eoo*, *eeo*, *ooe*, and *oee* spots change monotonically on rotation of the crystal, but the azimuths of the two remaining satellite spots do not. In fact, for *oeo* and *eoe* paths, Eqs. (6) become identical to those describing deflection of light by a prism of refractive index n_e/n_o and n_o/n_e, respectively, superposed on a horizontal deflection by 120°. Hence, on rotation of the crystal, the azimuthal distance, relative to the central spot, of the *oeo* and *eoe* spots passes through a minimum.

This minimum occurs for a symmetrical light path, in which case i_p at the first reflection and i_p' at the second reflection are equal.

D. Intensities

The intensities of the internally reflected rays can be calculated with Szivessy's formulas for the amplitude ratios of reflected and transmitted light.[6] For a birefringence as small as that of ice they approximate the Fresnel formulas. Hence the intensities of the reflected rays can be calculated efficiently from the Fresnel formulas with the aid of Mueller calculus,[10] considering the sequence: incoming totally linearly polarized light in one of the normal modes, (total) reflection, and decomposition of the new state of polarization into the two normal modes for the direction of propagation after reflection. The calculation yields four coefficients of reflection R, each of them conditional on the mode of the incoming ray (e or o ray) and on the mode of the reflected ray that one wishes to consider (e or o ray). We denote these coefficients by $R_{o\to e}$, $R_{o\to o}$, $R_{e\to o}$, and $R_{e\to e}$, where the first subscript indicates the mode of the incoming ray and the second the mode of the reflected ray under consideration. Thus $R_{o\to e}$ is the intensity of a reflected e ray created from an incident o ray of unit intensity, and so on.

For a prism face, the polarization angle η of the incident e ray (see Fig. 1) relates to γ and the angle of incidence, projected on a basal plane i_p, by

$$\tan i_p = \tan \eta \cos \gamma. \tag{7}$$

This leads to the following expressions for the four reflection coefficients R for total reflection at a prism face:

$$R_{o\to e} = R_{e\to o} = \frac{\sin^2(2i_p)\cos^2 \gamma}{1 - (1 + 1/n^2)\cos^2 i_p \sin^2 \gamma},$$
$$R_{o\to o} = R_{e\to e} = 1 - R_{o\to e}, \tag{8}$$

where n is the refractive index of ice. For plate orientation and the entrance of light at a basal face (the case we consider here), γ relates by Snel's law to h_{sun}:

$$\cos h_{\text{sun}} = n \sin \gamma. \tag{9}$$

For the parhelic circle, i_p relates directly to the azimuth Az with respect to the Sun by

$$\text{Az} = 180° - 2i_p. \tag{10}$$

Before and after the internal reflection, the (132) rays that generate the parhelic circle cross a basal face. The transmission coefficients T can be obtained from the usual Fresnel formulas for refraction. For extraordinary rays T is the coefficient for vertically polarized light, and for ordinary rays T is the coefficient of horizontally polarized light, so that

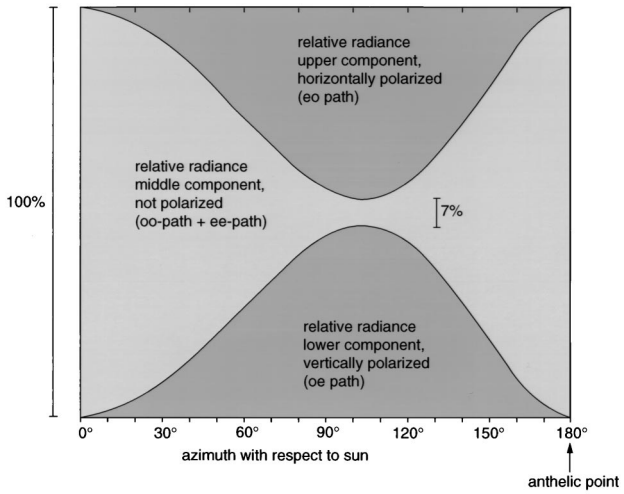

Fig. 3. Relative radiance of the three parhelic circle components as a function of azimuth. The upper component is completely horizontally polarized, the lower component is completely vertically polarized, and the middle component is virtually unpolarized. At azimuths between 90° and 120°, only the two polarized components have significant radiance. The plot is for solar elevation 35°, but the curves depend only weakly on solar elevation.

$$T_e(\text{basal face}) = 1 - \frac{\sin^2(90° - h_{\text{sun}} - \gamma)}{\sin^2(90° - h_{\text{sun}} + \gamma)},$$
$$T_o(\text{basal face}) = 1 - \frac{\tan^2(90° - h_{\text{sun}} - \gamma)}{\tan^2(90° - h_{\text{sun}} + \gamma)}. \tag{11}$$

The transmission coefficient of a ray through the whole crystal is then given by TRT; the indices of R and T depend on the polarization sequence. The distribution of the radiance as a function of azimuth over the three components of the parhelic circle is obtained by normalization of each product TRT with the sum over all components, which is

$$T_e R_{e\to o} T_o + T_e R_{e\to e} T_e + T_o R_{o\to o} T_o + T_o R_{o\to e} T_e$$
$$= T_e^{\,2} + T_o^{\,2} - (T_e - T_o)^2 R_{o\to e} \cong T_e^{\,2} + T_o^{\,2}. \tag{12}$$

This leads to the following relative radiances of the three parhelic circles:

upper and lower components (eo, oe paths)

$$= \frac{T_e T_o}{T_e^{\,2} + T_o^{\,2}} R_{o\to e} \cong 1/2 R_{o\to e},$$

middle component (ee + oo path) $\cong 1 - R_{o\to e}$. (13)

Figure 3 shows, for $h_{\text{sun}} = 35°$, the relative radiances as a function of azimuth. The middle component radiance is close to zero near an azimuth of 108°. A similar minimum appears for other solar elevations. The azimuth of this minimum decreases with solar elevation, but always remains between 90° and 120°. This implies that the parhelic circle shift in

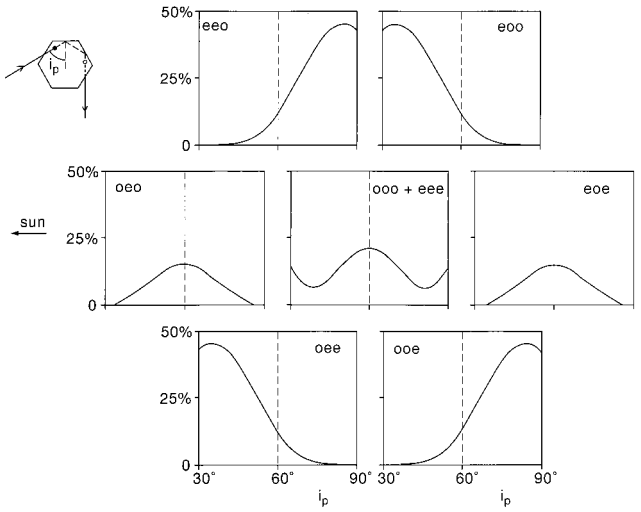

Fig. 4. Relative radiance of the seven 120° parhelion components as a function of projected angle of incidence i_p (abscissa) of the first reflection at a prism face. The graphs are arranged according to Fig. 2. The relative positions of the spots depend only weakly on i_p. The middle spot is the unpolarized component; its radiance is made up of two contributions (*ooo* and *eee*). The six other spots are all completely polarized (Fig. 2); their radiances consist of one contribution only (i.e., *eeo*, *eoo*, etc.). Note that the relative radiance patterns of diagonal pairs of spots are equal. At $i_p = 60°$ (dashed vertical lines) the ray path (neglecting splitting) is symmetrical with respect to the crystal hexagon. The plots are for a solar elevation of 35°, but for other elevations they are similar.

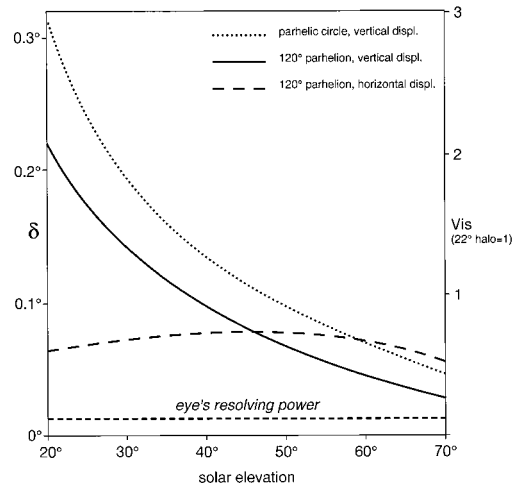

Fig. 5. Displacement δ of the parhelic circle and of the 120° parhelion when they are viewed through a rotating polarizer as functions of solar elevation. The parhelic circle displacement is vertical, and its value refers to the maximum displacement, which occurs at an azimuth between 90° and 120° from the Sun. The 120° parhelion shifts in both the horizontal and the vertical directions. The visibility Vis (right axis) of the displacements is defined as the displacement in units of that of the 22° halo.

polarized light is best observed in the region between 90° azimuth and the 120° parhelion.

The relative radiance of the seven constituent 120° parhelion spots is calculated in a similar way to that of the parhelic circle, the transmission coefficients through the crystal being of the form *TRRT*. The result depends strongly on the position of the crystal with respect to the incoming light ray: Rotation of a plate-oriented crystal about its vertical axis results in strong variations in the relative radiances. This is demonstrated in Fig. 4.

E. Broadening of the Radiance Profiles and Smearing

So far we have dealt with the idealized situation of ray optics, a perfect preferential crystal orientation, and a solar diameter of zero. The reality is different. Diffraction, imperfect crystal orientation, and the 0.5° solar-disk smearing will broaden the individual components to such an extent that they always largely overlap (see also the inset of Fig. 2). Hence only the limbs of the parhelic circle or the 120° parhelion remain noticeably polarized; the existence of polarized constituents can only be inferred from an up-and-down shifting of the phenomenon when viewed through a rotating polarizer and by an additional shifting in azimuth in the case of the 120° parhelion. As incoherent superposition is dominant when smearing leads to the recombination of differently polarized constituents, the directions of the limb polarizations can be directly linked to the polarization of the individual constituents of these halos.

The observed displacement δ of the parhelic circle in polarized light at a given azimuth equals the difference in height between the horizontally and the vertically polarized parhelic circle. The horizontally polarized circle consists of light from *eo* and *oo* paths. Its radiance is centered at a height that corresponds to the radiance-weighted mean position of its two constituents (*eo* and *oo* paths) under idealized conditions. Similarly, the center of radiance of the parhelic circle observed in vertically polarized light corresponds to the radiance-weighted mean height of the idealized parhelic circles from *oe* and *ee* paths. Using Eqs. (13) leads to

$$\delta = 2R_{o\to e}[h_p(oe) - h_{\text{sun}}], \tag{14}$$

where $h_p(oe)$ is given by the second formula of Eqs. (5). The displacement δ is maximal at the azimuth where the *oo* and the *ee* radiances are minimal; this happens for an azimuth that is between 90° and 120°. At that azimuth, $R_{o\to e}$ is 0.93 or more, so that δ amounts to almost twice the separation [Eqs. (5)] between the middle component of the circle and one of its satellite circles.

Similarly, the displacement δ of the 120° parhelion equals the difference in the radiance-weighted position of the horizontally (*ooo*, *eeo*, *eoo*, and *oeo* paths) and the vertically polarized constituents. In this case it makes sense to decompose the displacement into a vertical one and a horizontal one. The radiance-weighted position is obtained from the integral over i_p, taking into account the geometric shield-

ing factor F of 120° parhelion ray paths in thin regular hexagonal plates, which is

$$F(i_p, \gamma) = \cos(|i_p - 60°| + 60°) \times \cos(|i_p - 60°| - 60°)\sin\gamma \tan\gamma. \quad (15)$$

The displacement in azimuthal degrees, calculated with Eqs. (6), has to be multiplied by cos h_{sun} to obtain the horizontal displacement δ in great-circle degrees. We note that the horizontal 120° parhelion shift is exclusively due to the *oeo* and the *eoe* constituents, as the radiance-weighted i_p-averaged azimuths of the upper (*eeo* + *eoo*) and the lower (*ooe* + *oee*) spots are both exactly 120°.

Figure 5 shows the dependence of δ on solar elevation for the parhelic circle (maximum value) and the 120° parhelion. The right axis relates δ directly to a measure, Vis, of the visibility of the shift, where Vis = 1 at δ = 0.106°, which is the 22° halo shift.[2,3] The figure indicates a larger Vis for the parhelic circle displacement than for the vertical 120° parhelion displacement. However, the visibility of the shift also depends on the brightness of the halo and on its broadening, and Vis does not take those factors into account.

Smearing, by birefringence, of the parhelic circle and the 120° parhelion radiance may be detectable by an alert observer without the aid of a polarizer. It should be apparent by a bluish coloring of the halo edges. The reason is the 10% wavelength dependence of the birefringence $n_e - n_o$ over the visible spectrum.[7] The birefringence is largest for violet. Both the upper and the lower edges of a parhelic circle should have this bluish color; this (marginal) coloring is strongest where δ is maximal, i.e., somewhere between an azimuth of 90° and 120° from the Sun. Similarly, the blue coloring of the 120° parhelion boundary is strongest in its most polarized parts. The best chance to observe the blue color is in a bright parhelic circle or in a bright 120° parhelion with sharply defined edges. However, whether the color is in practice visible in nature remains to be checked.

3. Observations

A. Quartz Halos

During the long periods of absence of parhelic circles or 120° parhelia in the sky, their polarization effects can be studied by means of a polished piece of quartz cut in the shape of a hexagonal ice-crystal plate. The optic axis has to be perpendicular to the flat ends. Contrary to ice, quartz is optically active, but for $\gamma \lesssim 10°$ ($h_{\mathrm{sun}} \gtrsim 75°$) the optical activity of quartz becomes negligible[11] and the optical properties of ice and quartz are completely analogous. Hence halos generated by the polished quartz crystal behave as ice-crystal halos, but the separation between the polarized parhelic circle and 120° parhelion components is five times larger for quartz than that for ice. By inspection of the parhelic circle spots projected by the quartz crystal on a wall, it is immediately apparent that the ray path, which includes an internal reflection, is the dominating contribution to the parhelic circle radiance. For a fixed crystal position this contribution consists of three spots, two of which are totally polarized. This polarization is apparent when a polarizer is rotated in the light beam emerging from the crystal. Rotating the crystal about the optic axis causes the spots to form three circles. As shown for ice in Fig. 3, the intensities of the two polarized spots fade away when they approach the region of forward scattering, hence when their position is near the crystal's shadow. The same happens when the spots are near the point on the circle that is 180° separated from this. But when the position is 90°–120° from that shadow, the two polarized spots completely swamp the (unpolarized) one in the middle.

Fig. 6. Constituent spots of a 120° parhelion created by a nonrotating quartz crystal polished in the shape of an ice plate crystal. The picture was obtained by direct projection into a camera body without lens. The separation of the seven solar images is five times larger than that in ice (compare Fig. 2).

At 120° from the crystal shadow, there are a number of spots that are almost stationary during the crystal rotation. That is the 120° parhelion (see Fig. 6). On closer inspection, its seven components shift their relative positions somewhat during the crystal rotation, which is in accordance with Fig. 2, while the relative and absolute intensities of the spots vary markedly. It is easy to check that six of the seven spots are polarized, whereas the central spot is virtually unpolarized. It is instructive to see what happens when the incoming light is polarized with a second polarizer and how the intensities then vary when the polarizing filter in the emergent beam is rotated.

Further inspection of the emergent rays reveals the subparhelic circle and the 120° subparhelia, which behave similarly to their above-horizon counterparts. The number of halos that can be explored with such a quartz crystal is almost countless and each phenomenon has its own polarized surprise. We leave it to the readers to make their own discoveries.

B. Visual Observations on Real Halos

On three occasions one of us (GPK) had the opportunity to search for polarization effects in real parhelic circles and 120° parhelia.

The first and the second occasions occurred at the U.S. Amundsen–Scott South Pole station during the 1989–1990 austral summer season, on 2 and 6 January, respectively. The solar elevations were 23°

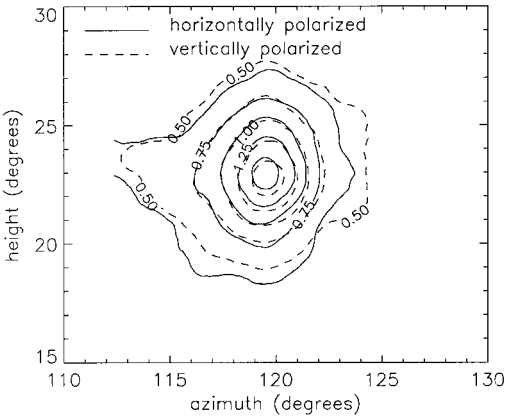

Fig. 7. Observed radiance of the 120° parhelion for horizontal and vertical polarization (arbitrary units). The background has been subtracted; see Subsection 3.C for further details. The 120° parhelion in horizontal polarization is 0.2° higher in the sky and 0.1° closer to the Sun (concentrate on the inner three contours, where both the radiance and its gradient are maximum). The lobe to the left results from a weakly developed parhelic circle. The observation took place on 6 January 1990 at the U.S. Amundsen–Scott South Pole station. The solar elevation was 22.5°.

and 22.5°. On these days the radiance of the plate halos was enormous and a try was worthwhile. Actually, GPK concentrated on the 120° parhelion, as he was still unaware that the parhelic circle might show even stronger polarization if viewed at the correct azimuth. GPK managed to see the vertical 120° parhelion shift, not the horizontal one. The observation of the shift proved to be unexpectedly difficult. With hindsight, this can be explained by the rather diffuse appearance of South Pole low-level halos, which we attribute to smearing due to variations in the interfacial angles of crystals in growing conditions.[3] The picture of the 2 January display in Plate 22 of Ref. 3 shows a 3° diameter of the 120° parhelion.

The third occasion was on 24 August 1995 at approximately 15:40 local time on the Dutch island of Terschelling at 42° solar elevation. Contrary to typical South Pole displays, here the parhelic circle and 120° parhelion were sharply defined. The shifting positions of the parhelic circle and the 120° parhelion, both in the vertical and in the horizontal direction, were clearly seen through the rotating polarizer; the visibility of the parhelic circle shift and that of the vertical and the horizontal shifts of the 120° parhelion were about the same. This agrees approximately with Fig. 5. We note that the radiance of the parhelic circle was lower than that of the 120° parhelion; this may explain the lack of excess visibility (as predicted by Fig. 5 for $h_{\mathrm{sun}} = 42°$) of the parhelic circle shift relative to that of the 120° parhelion.

C. Quantitative Observation

On 6 January 1990 we managed to catch a 120° parhelion with our polarimetric camera.[2–3] The location of observation was the U.S. Amundsen–Scott South Pole Station, 20:13 local time at a solar elevation of 22.5°. The 120° parhelion appeared in a low-level ice-crystal swarm. No crystals were sampled during this short-lived display. At this 120° parhelion the vertical displacement in polarized light was also checked visually (Subsection 3.B). The data handling of the digitized negatives was as described before[3]; a running 1° × 1° smoothing was applied. The overall 120° parhelion polarization was vertical, and the intrinsic degree of polarization at its radiance maximum was 6.5%, which agrees within the experimental uncertainty with the 8% value that follows from the Fresnel coefficients of refraction [Eqs. (11)] of the seven constituent components. In the representation of the radiance fields (Fig. 7) the background radiance (4.5 in the units of Fig. 7) has been subtracted and the intrinsic halo polarization has been removed by multiplication the halo radiances in the two polarization channels by factors of 1.065 and 0.935.

Figure 7 shows the resulting 120° parhelion radiance fields for horizontal and vertical polarization. The 1.2 contour has a diameter of ~3°, which corresponds to the visual diameter of the 120° parhelion on the photographic negative and in the sky. The extension of the contours to the left, which is due to a weakly developed parhelic circle, indicates a tilt of the camera of ~4°. Such an offset is quite possible because the spirit level of the camera could not be used.

Figure 7 clearly shows the displacement of the 120° parhelion in polarized light. The shift is most apparent in the inner three contours, where the radiance gradient is highest. (The displacement of the outer contours, e.g., the 0.5 contour, is probably also due to variations in polarization of the 4.5 background radiance caused by inhomogeneities in density of the crystal cloud and cannot be trusted for detection of the 120° parhelion shift; in the inner parts of the parhelion this disturbing effect becomes of minor importance.) The displacement is absent in the inner contours of the other channels of the camera (polarization angles ±45°, not shown), as it should be. The magnitude of the displacement in Fig. 7 is 0.2° in the vertical and ~0.1° in the horizontal, which agrees with Fig. 5.

4. Conclusions

- Parhelic circles from plate-oriented ice crystals and 120° parhelia move when viewed through a rotating polarizer.
- The maximum parhelic circle shift occurs at an azimuthal distance between 90° and 120° from the Sun.
- In horizontal polarization the parhelic circle and 120° parhelion are shifted upward.
- The magnitudes of the vertical shifts decrease with increasing solar elevation, but are visible to the eye for sharply defined halos up to a solar elevation of at least 40°.
- The 120° parhelion also shifts in horizontal position. In horizontally polarized light, it is closest to the Sun.

• The horizontal shift depends weakly on solar elevation and is visible to the eye for sharply defined 120° parhelia.
• The light of the limbs of a parhelic circle and a 120° parhelion should have a bluish coloring; the coloring will be strongest where the limb polarization is largest. For sharply defined edges the coloring may be visible to the naked eye.
• No displacements or coloring occur for parhelic circles generated by crystal orientations with the main axis horizontal. This applies to parhelic circles due to column orientation and Parry orientation.

This research was supported by National Science Foundation grant DPP-8816515 and partly by the Antarctic Program of the Netherlands Organization for Scientific Research.

References and Notes

1. G. P. Können, "Polarization of haloes and double refraction," Weather **32,** 467–468 (1977).
2. G. P. Können and J. Tinbergen, "Polarimetry of a 22° halo," Appl. Opt. **30,** 3382–3400 (1992).
3. G. P. Können, S. H. Muller, and J. Tinbergen, "Halo polarization profiles and the interfacial angles of ice crystals," Appl. Opt. **33,** 4569–4579 (1994).
4. G. P. Können, "Identification of odd-radius halo arcs and of 44°/46° parhelia by their inner-edge polarization," Appl. Opt. **37,** 1450–1456 (1998).
5. W. Tape, *Atmospheric Halos*, Vol. 64 of Antarctic Research Series (American Geophysical Union, Washington, D.C., 1994).
6. G. Szivessy, "Kristaloptik," in *Handbuch der Physik*, H. Konen, ed. (Springer, Berlin 1928), Vol. 20, p. 702 and pp. 715–718.
7. H. E. Merwin, "Refractivity of birefringent crystals," in *International Critical Tables*, E. W. Washburn, ed. (McGraw-Hill, New York, 1930), Vol. 7, pp. 16–33.
8. W. Snel van Royen (Leiden, Netherlands 1580–1626), latinized name Snellius, is often incorrectly retranslated as Snell. See also Ref. 9.
9. W. D. Bruton and G. W. Kattawar, "Unique temperature profiles for the atmosphere below an observer from sunset images," Appl. Opt. **36,** 6957–6961 (1997); see authors' note in Ref. 5.
10. E. Collett, *Polarized Light: Fundamentals and Applications* (Marcel Dekker, New York, 1993).
11. P. Drude, "Rotationspolarisation," in *Handbuch der Physik*, A. Winkelman, ed. (Barth, Leipzig, 1906), Vol. 4, pp. 1347 and 1353.